



Mechanism of Baicalein in Brain Injury After Intracerebral Hemorrhage by Inhibiting the ROS/NLRP3 Inflammasome Pathway

Xuan Chen¹, Yue Zhou², Shanshan Wang³ and Wei Wang^{4,5} 

Received 9 June 2021; accepted 17 September 2021

Abstract—Intracerebral hemorrhage (ICH) is a devastating subtype of stroke with high disability/mortality. Baicalein has strong anti-inflammatory activity. This study aims to explore the mechanism of baicalein on brain injury after ICH. The model of brain injury after ICH was established by collagenase induction, followed by the evaluation of neurological severity, brain water content, the degenerated neurons, neuronal apoptosis, and reactive oxygen species (ROS). The ICH model was treated with baicalein or silencing NLRP3 to detect brain injury. The expression of NLRP3 inflammasome was detected after treatment with ROS scavenger. The expressions of oxidative stress markers and inflammatory factors were detected, and the levels of components in NLRP3 inflammasome were detected. Baicalein reduced the damage of nervous system, lesion surface, brain water content, and apoptosis. Baicalein inhibited malondialdehyde and increased IL-10 by inhibiting ROS in brain tissue after ICH. Baicalein inhibited the high expression of NLRP3 inflammasome in ICH. ROS scavenger inhibited the NLRP3 inflammatory response by inhibiting ROS levels. Silencing NLRP3 alleviated the brain injury after ICH by inhibiting excessive oxidative stress and inflammatory factors. Overall, baicalein alleviated the brain injury after ICH by inhibiting ROS and NLRP3 inflammasome.

KEY WORDS: baicalein; brain injury; intracerebral hemorrhage; NLRP3 inflammasome; reactive oxygen species; neuron

¹Department of Neurosurgery, The First People's Hospital of Shangqiu, No. 292 Kaixuan Road, Suiyang District, Shangqiu, Henan, China

²Department of Neurological Rehabilitation, Yidu Central Hospital, Weifang, China

³Department of Cardiology First Ward, Yidu Central Hospital, Weifang, China

⁴Department of Neurology, The Fourth Affiliated Hospital of China Medical University, 4 Chongshan East Street, Shenyang 110032, China

⁵To whom correspondence should be addressed at Department of Neurology, The Fourth Affiliated Hospital of China Medical University, 4 Chongshan East Street, Shenyang, 110032, China. Email: wanwei0311@163.com

INTRODUCTION

Intracerebral hemorrhage (ICH) is a cerebrovascular disease with extremely high disability and mortality rates, while existing treatments have many limitations [1, 2]. A series of inflammatory responses including neuroinflammation, apoptosis, and oxidative stress after ICH promote secondary brain injury after ICH, and this secondary injury is the key factor of ICH-induced brain injury [3]. Therefore, research on effective methods to reduce and eliminate secondary brain injury caused by

inflammation has become the focus and challenge of current brain injury treatment after ICH.

Baicalein is the main active component isolated from the root of *Scutellaria baicalensis*, which has strong anti-inflammatory activities through a multi-target mechanism [4]. A previous study has shown that baicalein can reduce the volume of brain lesions, brain water content, the level of pro-inflammatory cytokines, and the number of apoptotic cells, increase the activity of superoxide dismutase (SOD) and glutathione peroxidase (GSH-Px) in rat brain tissue, and reduce the level of malondialdehyde (MDA) [3]. Baicalein also has been shown to promote neuronal and behavioral recovery after ICH by inhibiting apoptosis, oxidative stress, and neuroinflammation, and can be developed as a new drug for the clinical treatment of ICH and brain injury related to ICH [3]. Recently, it has been documented that acute liver injury can be alleviated by baicalein by inhibiting the nucleotide-binding domain-like receptor protein 3 (NLRP3) inflammasome [5]. Baicalein reversed neuroinflammation in rats by inhibiting the NLRP3/caspase-1/gasdermin D pathway [6]. Both the activation of NLRP3 inflammasome and reactive oxygen species (ROS) could be downregulated by baicalein [7]. These results indicated that NLRP3 inflammasome could be inhibited by baicalein.

NLRP3 inflammasome is a multi-molecular complex that is crucial in innate immunity [8]. Its activation can further promote the occurrence of inflammation, enhance the host's ability to remove pathogens, and promote the repair of damaged tissues, but if the activation of inflammasome is disordered, it will cause the development of various inflammatory diseases and metabolic disorders [9]. NLRP3 inflammasome-mediated apoptosis is crucial in cerebral ischemia/reperfusion (I/R) injury [10]. Inhibition of NLRP3 inflammasome activation ameliorates acute inflammatory injury induced by necrotizing enterocolitis in rats [11]. NLRP3 inflammasomes is crucial in the inflammatory process that occurs in ICH-induced injury [12]. NLRP3 inflammasomes can be activated after ICH, leading to inflammatory cascade reaction and aggravating brain injury [13]. Blocking NLRP3 may be a therapeutic target for ICH recovery [14]. ROS plays an important role in the activation of NLRP3 inflammasomes [15]. A previous study has reported that anti-inflammatory properties of melatonin may inhibit the activation of ROS-NLRP3 inflammasome and protect hippocampal neuron cells against apoptosis after ICH [8]. Many scholars have studied the effect of NLRP3 inflammasomes on brain injury after ICH.

However, the mechanism of baicalein in brain injury after ICH by regulating the ROS/NLRP3 inflammasome signaling has not been reported. Therefore, this study set out to identify the mechanism of baicalein inhibiting the ROS-NLRP3 inflammasome in brain injury after ICH.

MATERIALS AND METHODS

Ethics Statements

Animal experiments followed the standards established by the animal experiment committee of the Fourth Affiliated Hospital of China Medical University and approved by the ethics committee of the Fourth Affiliated Hospital of China Medical University. All animal experiments were conducted according to the "Guidelines for the Care and Use of Laboratory Animals" [16].

Intracerebral Hemorrhage (ICH) Model Establishment

The ICH model was established in 48 female Sprague–Dawley rats (8 weeks old) purchased from Hunan SJA Laboratory Animal Co., Ltd (Hunan, China).

The ICH model was processed according to the literature [17], and the specific procedure was as follows: stereotactic intranasal injection of type VII collagenase (Sigma-Aldrich, St. Louis, Missouri, USA). After anesthesia, a burr hole was drilled at the injection site (3.0 mm left of the midline, 0.2 mm posterior to the bregma, and 6 mm below the skull) and type VII collagenase (dissolved in 0.23 μ L brine) was slowly injected at a rate of 0.5 μ L/min into the central striatum. Then, the needle was kept at the injection site for another 10 min to prevent reflux. The skull was sealed using bone wax after craniotomy. Rats were assigned into the sham group, ICH group, ICH + dimethyl sulfoxide (DMSO) group (treated with DMSO after the rat ICH modeling), ICH + baicalein group (treated with 50 mg/kg baicalein after the rat ICH modeling), ICH + H₂O group (treated with H₂O after the rat ICH modeling), ICH + N-acetylcysteine (NAC) group (treated with 5 mM NAC after the rat ICH modeling) [18], ICH + sh-negative control lentivirus (sh-NC) group (treated with sh-NC after the rat ICH modeling), and ICH + sh-NLRP3 group (treated with sh-NLRP3 after the rat ICH modeling), with 6 rats per group. The treatments of sh-NC, oe-NC, sh-NLRP3, and oe-NLRP3 were as follows [16]: rats were given stereotactic microinjection of

lentivirus particles at a dose of 2.0 μL (10–10 TU/mL) into the CAI region of the right hippocampus, 72 h before ICH treatment. The treatments of H_2O and baicalein were as follows: the same volume (1 mL) of H_2O or baicalein was injected intraperitoneally at an interval of 12 h for 3 days. After 1 and 3 days of baicalein treatment, the rats were subjected to neurology score evaluation. After 3 days of baicalein treatment, the rats were euthanized with excessive sodium pentobarbital. Half of the tissues were used for brain edema assessment, and the other half were used for histological staining, quantitative reverse transcription polymerase chain reaction (qRT-PCR) and western blot (WB).

Modified Neurological Severity Score (mNSS)

To assess neurological abnormalities in animals, a mNSS [19] was performed by two independent investigators who were unaware of the experimental treatment. The mNSS test is composed of motor, sensory, reflex, and balance tests. Neurological function scores ranged from 0 to 18 according to supplementary table 1 (normal = 0; maximum defect score = 18).

Assessment of Cerebral Edema

After euthanizing animals with an overdose of pentobarbital sodium (160 mg/kg body weight) [20], the brains were removed and divided into the contralateral and ipsilateral hemispheres and the cerebellum. Each tissue was weighed immediately to obtain a wet weight and then dried at 160 °C for 24 h to obtain a dry weight. The formula for calculating water content was as follows: $[(\text{wet weight} - \text{dry weight}) / (\text{wet weight})] \times 100\%$.

Fluoro Jade—c (FJC) Staining

The number of degenerated neurons was assessed by FJC staining. ICH sections were detected using FJC's standby dilution staining kit (Biosensis Pty Ltd, Thebarton, South Australia). After rinsing with phosphate buffer saline (PBS), the sections were incubated in FJC working solution for 20 min according to the instructions, and then observed under a fluorescence microscope. The number of FJC-positive neurons was calculated as follows: three brain regions of the microscope field around hematoma were randomly selected from each rat and then

the number of FJC-positive neurons was calculated using the ImageJ software (NIH, Bethesda, MD, USA).

TUNEL Staining

Apoptosis was detected by TUNEL staining. In brief, sections were paraffined, dewaxed, hydrated, and cleared in brain tissues in different treatment groups. The TUNEL staining reaction solution (Roche, Shanghai, China) was added and the apoptotic cells were calculated under the fluorescence microscope (Eclipse Ti-U, Nikon Co, Japan) and photographed.

Nissl Staining

The brain tissues were paraffined and rehydrated, and stained with Nissl staining solution (Beyotime, C0117) at 50–60°C for 40 min. After, the tissues were washed with distilled water, recrystallized with gradient ethanol, and then cleared in 100% dimethylbenzene for 5 min. Then, the tissues were sealed with neutral gum or other sealant. The tissues were observed under the light microscope.

Hematoxylin–Eosin (HE) Staining

After embedding the tissue, the wax block was fixed on a conventional continuous section with a thickness of 4 μm . The wax block was spread and pasted in water at 46°C, and then baked in a toaster at 72°C for 2 h. The sections were cooled for 10 min, then dewaxed with xylene I for 10 min, dewaxed with xylene II for 10 min, fixed with anhydrous ethanol I and II for 5 min, with 90% ethanol for 2 min, with 80% ethanol for 2 min, and fixed with 70% ethanol for 2 min, and flushed with water for 5 min, and stained with hematoxylin for 5–10 min. Next, the sections were flushed with water for 5 min, differentiated with hydrochloric acid alcohol for 2–3 s, blued with lithium carbonate for 10 min, stained with eosin for 2 min, dehydrated with 80% ethanol for 2 min, with 90% ethanol for 2 min, with anhydrous ethanol for 2 min, and cleared with xylene for 2 min. The sections were finally wiped, sealed with neutral resin, and observed under the microscope.

Immunohistochemistry

The specimens were fixed with 10% formaldehyde, and paraffined embedded were sliced at 4 μm . The tissue

sections were baked at 60 °C for 1 h, dewaxed with conventional xylene, then dehydrated with gradient alcohol, incubated at 37 °C in 3% H₂O₂ (Sigma) for 30 min, washed with PBS, and boiled in 0.01 M citrate buffer at 95 °C for 20 min, then cooled to room temperature, and washed with PBS. The tissue sections were sealed with normal sheep serum working solution for 37 °C for 10 min. Sections were incubated with NLRP3 (ab214185; 1:200, Abcam, Cambridge, MA, USA), caspase-1 (ab62698, 1:500, Abcam), and IL-1 β (ab216995, 1:200, Abcam) antibodies at 4 °C for 12 h. After washing with PBS, the corresponding biotin-labeled goat anti-rabbit secondary antibody was added, and the reaction was carried out for 10 min. After washing thoroughly, horseradish peroxidase labeled streptomycin working solution (S-A/HRP) was added to react at room temperature for 10 min. The sections were visualized using diaminobenzidine and stored in a dark room for 8 min. The sections were rinsed with tap water, stained with hematoxylin, dehydrated, cleared, sealed, and observed under light microscope. Nikon Imaging Software was used to count the positive cells. Three non-overlapping fields of equal area (200 \times) were selected from each section to count the number of positive cells.

Immunofluorescence

The slides were fixed with 4% paraformaldehyde for 15 min, soaked in PBS 3 times, and dried with absorbent paper. Normal goat serum was added to the slides and sealed at room temperature for 30 min. The blocking liquid on the slides was absorbed with absorbent paper and the slides without washing. The primary antibodies NLRP3, Caspase-1, and apoptosis-associated speck-like (ASC) were added to each slide for overnight incubation at 4 °C. The slides were dipped and washed three times with phosphate buffered saline with 0.05% Tween 20, 3 min each, and incubated with Alexa Fluor 488 labeled goat anti-rabbit IgG (ab150077, Abcam, UK) and Alexa Fluor 647 labeled goat anti-rabbit IgG (ab150083, Abcam) at 37 °C for 1 h in the dark. After rinsing the slides with PBS 3 times in the dark, stain with 5 μ g/mL DAPI for 5 min and then wash with PBS for 5 min 3 times. Slides were sealed and stored at 4 °C in the dark. The results were observed with the software Nis-Elements Viewer using a confocal laser microscope (Zeiss LSM 510, Zeiss, Oberko, Germany).

Determination of Reactive Oxygen Species (ROS)

The slides were fixed with 4% paraformaldehyde for 15 min, and then soaked with PBS for 3 times. The PBS was dried with absorbent paper, and normal goat serum was added to the slides and then the slides were sealed at room temperature for 30 min. The blocking solution was absorbed by absorbent paper without washing. Each slide was dripped with 2',7'-dichlorodihydrofluorescein diacetate (DCF-DA) diluent and incubated at 37 °C for 30 min, and observed under a light microscope (Olympus, Tokyo, Japan). Fluorescence intensity was evaluated using Image Pro Advanced 6.0 software (NIH, Bethesda, MD, USA).

Enzyme-Linked Immunosorbent Assay (ELISA)

The expression of inflammatory cytokine interleukin-1 (IL-1) (1,210,122, IL-1 β ELISA kit 96 T, Dakewe, Shenzhen, China), tumor necrosis factor- α (TNF- α) (1,217,202, TNF- α ELISA kit 96 T, Dakewe), and IL-10 (1,311,002, IL-10 ELISA kit 96 T, Dakewe) in serum of rats was detected. The levels of MDA, SOD, and GSH-Px in the serum of rats were also measured according to the instructions of ELISA kits (Bio-Swamp, Wuhan, China). Specific steps can refer to the operation manual. Briefly, 100 μ L antibody dilution buffer was incubated with the biotinized antibody working solution (1:100, 100 μ L/well) for 2 h, the value of optical density (OD) was measured at 450 nm, and the results were obtained by comparing with the standard and blank control. The experiment was repeated 3 times.

qRT-PCR

Total RNA was extracted using TRIzol (Invitrogen, Car, USA). RNA was reverse transcribed into cDNA using PrimeScript RT kit (RR037A, Takara, Japan). The reaction system was 10 μ L. Then, the reaction solution was taken for fluorescence quantitative PCR according to the instructions of the SYBR®Premix ExTaq™ II kit (RR820A, TaKaRa) using a real-time quantitative fluorescence PCR system (ABI 7500, ABI, Foster City, CA, USA). Using GAPDH as an internal reference, the relative expression of each target gene was calculated by the 2^{- $\Delta\Delta$ Ct} method [21]. The relevant primers were designed by Shanghai Sangon Bio (Shanghai, China) (Table 1).

Table 1 Primer Sequence

Gene	Primer sequences
NLRP3	F: 5'-AGCCTCAACAAACGCTACAC-3' R: 5'-CATCATCGGGGTCAAACAG-3'
IL-1 β	F: 5'-GCAGCTATGGCAACTGTT-3' R: 5'-GAGCCTGTAGTGCAGTTGTC-3'
ASC	F: 5'-GGAGTCGTATGGCTTGGAGC-3' R: 5'-CGTCCACTTCTGTGACCCTG-3'
GAPDH	F: 5'-AATCCCATCACCATCTTC-3' R: 5'-AGGCTGTTGCATACTTC-3'

Western Blot (WB)

Tissues were collected by trypsin digestion and lysed with the enhanced radio immunoprecipitation assay lysate (Boster, Wuhan, China) containing protease inhibitors, and then the protein concentration was determined with the bicinchoninic acid protein quantitative kit (Boster, Wuhan, China). Proteins were isolated with 10% SDS-PAGE, and the isolated proteins were transferred to polyvinylidene fluoride membranes. The membranes were sealed with 5% bovine serum albumin for 2 h to block non-specific binding. Diluted primary antibodies NLRP3 (ab214185, 1:1000, Abcam), Caspase-1 (ab62698, 1:1000, Abcam), ASC (ab180799, 1:1000, Abcam), and GAPDH (ab9485, 1:2500, Abcam) were added, respectively, and incubated overnight at 4°C. After washing the membranes, HRP-labeled sheep anti-rabbit secondary antibody (ab6721, 1:2000, Abcam) was added into the membranes and incubated for 1 h. Next, the membranes were added with enhanced chemiluminescence (ECL) working solution (EMD Millipore, MA, USA) at room temperature for 1 min. Then the excess ECL reagent was removed, the membranes were sealed with the plastic wrap, and X-ray film was put in the dark box for 5–10-min exposure for blotting development and fixation. ImageJ analysis software (NIH) was used to quantify the grayscale of each band in Western blot images, and GAPDH was used as an internal reference. Each experiment was repeated 3 times.

Statistical Analysis

SPSS version 19.0 (IBM Corp. Armonk, NY, USA) was used for statistical analysis. All data were in compliance with normal distribution and homogeneity of variance. Data were presented as mean \pm standard deviation.

Unpaired *t* test was used to compare the data between two groups, and one-way analysis of variance (ANOVA) was used to compare the data among multiple groups. Tukey's was used for post hoc test. A value of $P < 0.05$ indicated the difference was statistically significant.

RESULTS

Baicalein Reduced Brain Injury After ICH

Baicalein has therapeutic effects on brain injury [3]. To explore the mechanism of baicalein on brain injury after ICH, we established a brain injury model after ICH by collagenase induction. The mNSS was used for neurological assessment. The neurological damage of ICH group was worse than that in the sham group (Fig. 1A). Brain water content was measured by dry/wet method, and the results showed that brain water content in the ICH group was significantly increased (Fig. 1B). The number of degenerated neurons was detected by FJC, which showed that the degenerated neurons in the ICH group were clearly increased (Fig. 1C). Meanwhile, TUNEL staining showed that the apoptosis in the ICH group was increased (Fig. 1D). Nissl staining showed that the Nissl bodies in the ICH group were evidently reduced (Fig. 1E). HE staining was used to detect the pathological conditions of brain tissue, which showed that the pathological severity of the ICH group was significantly increased (Fig. 1F). These results indicated that the animal model of ICH was successfully established, and there was brain injury after ICH. Then we treated the ICH rat model with baicalein and scored each rat with mNSS. Compared with the ICH + DMSO group, the ICH + baicalein group had neurological injury, and the lesion volume and brain water content were reduced, cell apoptosis was reduced, the number of Nissl bodies was increased, and the severity of pathology was significantly reduced (Fig. 1A–F). The above results indicated that baicalein treatment can improve brain injury after ICH.

Baicalin Inhibited Brain Injury After ICH Caused by ROS Oxidative Stress

In order to explore the mechanism of baicalein on the improvement of ICH brain injury, DCF fluorescence staining was used to detect the ROS expression levels in brain tissues. Compared with the sham group, ROS level in the ICH + baicalein group was increased, and compared with the ICH + DMSO group, ROS level

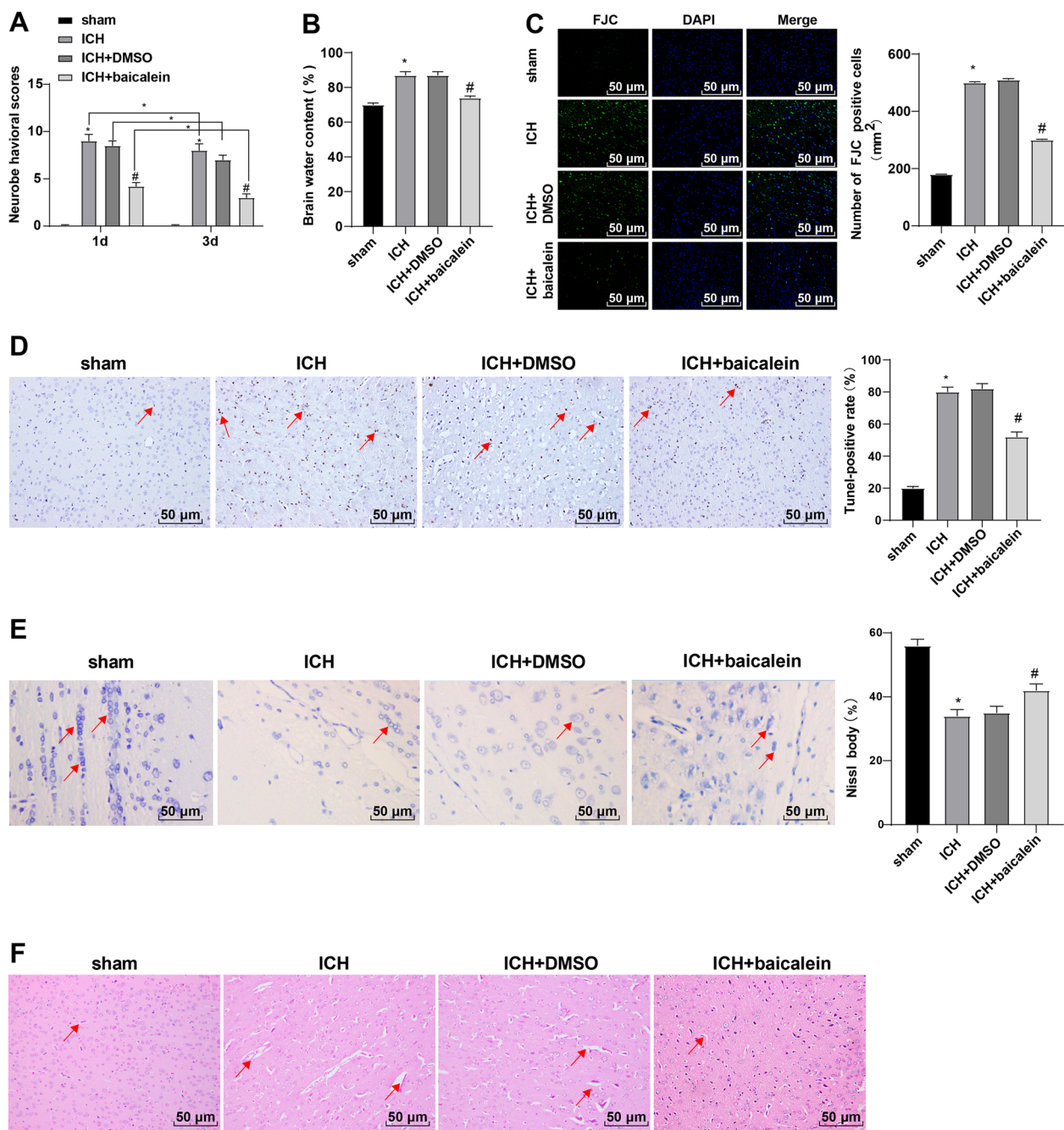


Fig. 1 Baicalein reduced brain injury after ICH. **A** The mNSS was used to score the neurological severity. **B** Brain water content measured as a percentage of wet/dry weight. **C** The number of degenerated neurons was detected by FJC staining (magnification: ×200). **D** TUNEL staining was used to detect brain tissue apoptosis (magnification: ×200, yellow–brown area indicated by the arrow was indicative of TUNEL-positive). **E** Nissl staining was used to detect the condition of Nissl bodies (magnification: ×200, blue-purple areas indicated by the arrows represent positive Nissl bodies). **F** HE staining was used to detect the pathological condition of brain tissue (magnification: ×200, the areas indicated by the arrows represent vacuoles, shrinkage, inflammatory cell infiltration in brain tissue). Data were presented as mean ± standard deviation, and unpaired *t* test was used for comparison between two groups (*N* = 6). * compared with the sham group, *P* < 0.05, # compared with the ICH + DMSO group, *P* < 0.05.

was significantly decreased in the ICH + baicalein group (Fig. 2A). ELISA was used to detect oxidative stress markers in serum of rats. Compared with the sham group, MDA content in ICH group was obviously enhanced, and SOD and GSH-Px activities were significantly decreased. Compared with the ICH + DMSO group, the expression of MDA in ICH + baicalein group was significantly decreased, and the activities of SOD and GSH-Px were significantly increased (Fig. 2B–D). In short, the brain injury caused by oxidative stress and inflammation factors can be reduced by baicalein.

NLRP3 Inflammasome Was Inhibited by Baicalein

The NLRP3 inflammasomes can be inhibited by baicalein, and ROS levels can also be reduced by baicalein, and the inflammation mediated by NLRP3 inflammasomes can be inhibited by ROS scavenger NAC [4, 6, 7, 18, 22]. To investigate whether

baicalein inhibited brain injury after ICH by affecting NLRP3 inflammasome, we detected the levels of NLRP3, ASC, and caspase-1 in ICH brain tissue by RT-qPCR and WB. Compared with the sham group, the levels of NLRP3, ASC, and caspase-1 in the ICH group were increased, but significantly reduced in the ICH + baicalein group compared with the ICH + DMSO group (Fig. 3A, B). Meanwhile, the levels of NLRP3, caspase-1, and IL-1 β were detected by IHC, which showed that compared with the sham group, these protein levels in the ICH group were significantly increased, but significantly decreased in the ICH + baicalein group when compared with the ICH + DMSO group (Fig. 3C). ELISA showed that compared with the sham group, IL-1 β and TNF- α were elevated and IL-10 was diminished in the ICH group, and compared with the ICH + DMSO group, IL-1 β and TNF- α were decreased and IL-10 was elevated in the ICH + baicalein group (Fig. 3D–F). The above results indicated that baicalein can inhibit the high expression of NLRP3 inflammasome in ICH.

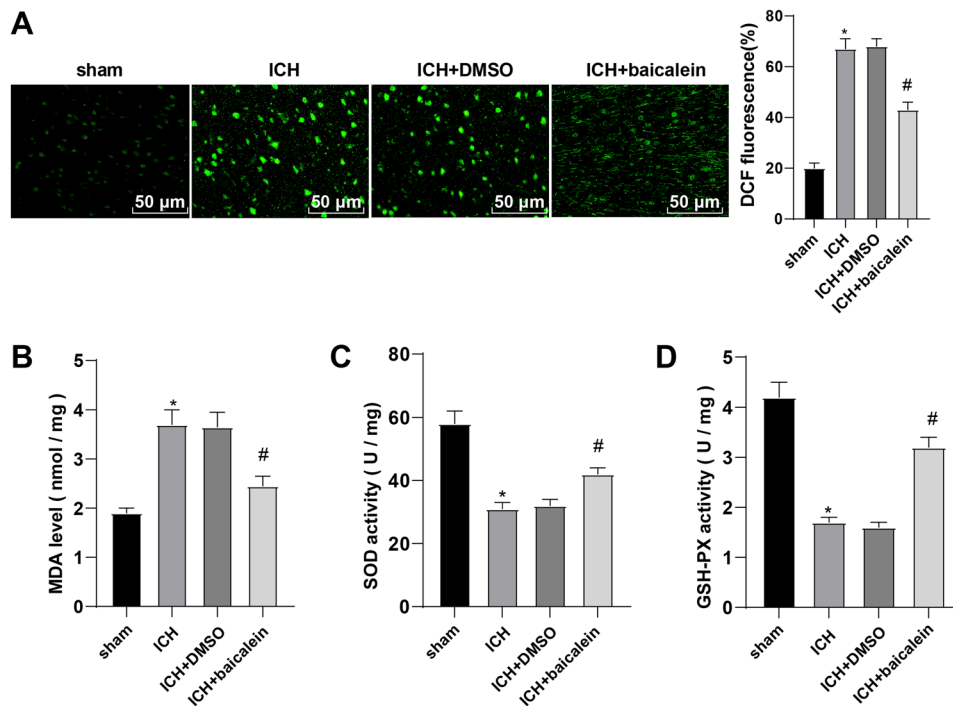


Fig. 2 Baicalein inhibited brain damage after ICH induced by ROS. **A** DCF fluorescence staining was used to detect ROS expression levels in brain tissues of rats in each group (magnification: $\times 200$). **B–D** The expression levels of MDA, SOD, and GSH-Px in serum were detected by ELISA. Data were presented as mean \pm standard deviation, and unpaired *t* test was used for comparison between two groups ($N=6$). * compared with the sham group, $P < 0.05$; # compared with the ICH + DMSO group, $P < 0.05$.

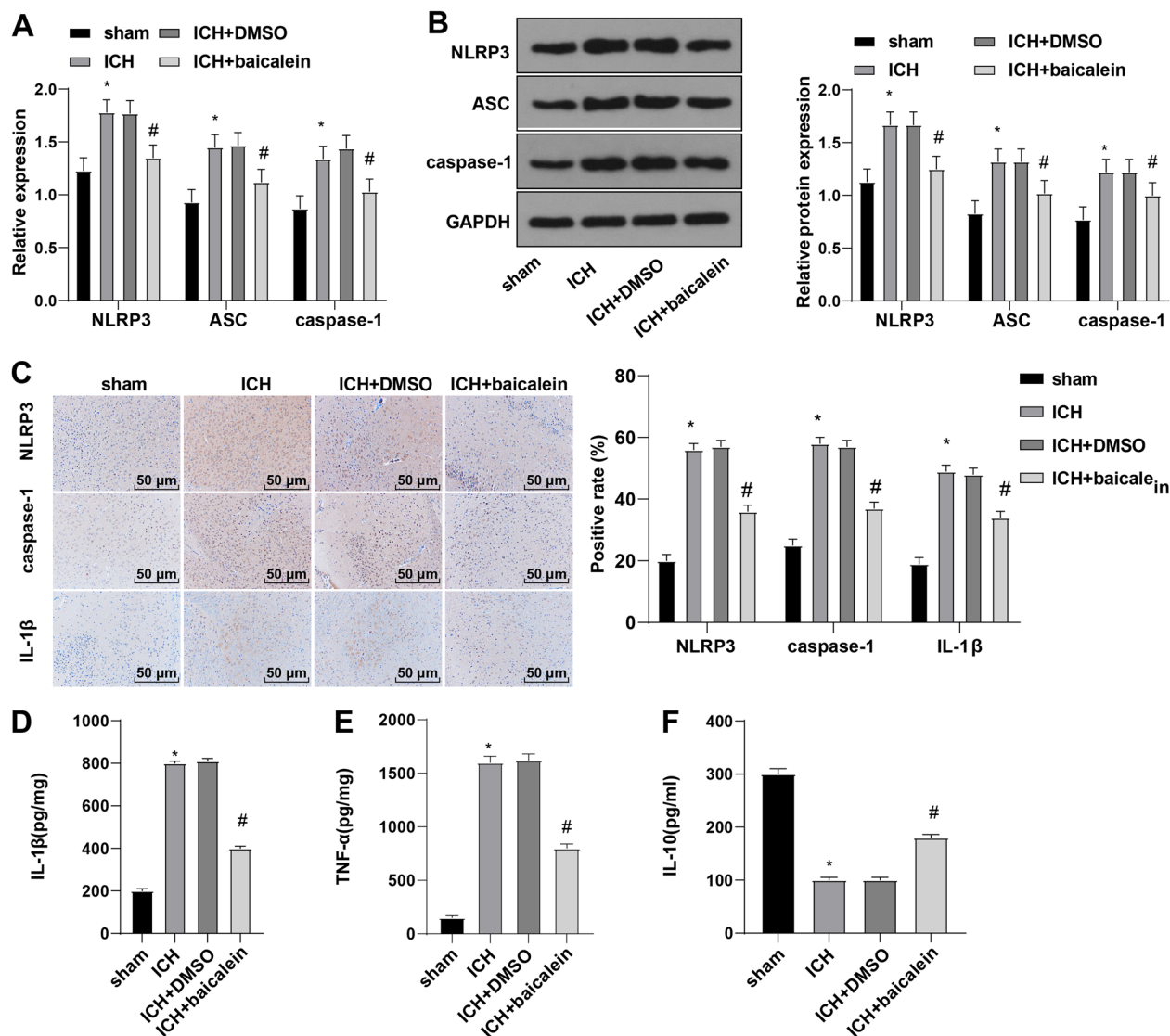


Fig. 3 Baicalein inhibited the expression of NLRP3 inflammasome. **A** qRT-PCR was used to detect the mRNA expression levels of NLRP3, ASC, and caspase-1 in the brain tissues of rats in each group. **B** WB was used to detect the protein levels of NLRP3, ASC, and caspase-1 in brain tissue of ICH rats. **C** The expression levels of NLRP3, Caspase-1, and IL-1β in brain tissues of rats in each group were detected by immunohistochemistry (magnification: ×200). **D–F** The expression levels of inflammatory cytokines IL-1β, TNF-α, and IL-10 in serum of rats were detected by ELISA. Data were presented as mean ± standard deviation, and unpaired *t* test was used for comparison between two groups (*N* = 6). * compared with the sham group, *P* < 0.05; # compared with the ICH + DMSO group, *P* < 0.05.

ROS Scavenger NAC Inhibited NLRP3 Inflammasome-Mediated Inflammation

To investigate the effect of ROS on NLRP3 inflammasomes, we tested relevant indicators after the treatment of ICH with ROS scavenging agent (NAC). DCF fluorescence staining was used to detect ROS expression levels.

Compared with the ICH + H₂O group, ROS level in the ICH + NAC group was significantly decreased (Fig. 4A). ELISA was used to detect oxidative stress markers. Compared with the ICH + H₂O group, MDA expression in the ICH + NAC group was significantly decreased, while SOD and GSH-Px activities were significantly increased (Fig. 4B–D). WB showed that NLRP3, ASC,

and caspase-1 proteins were significantly downregulated in the ICH+NAC group compared with the ICH+H₂O group (Fig. 4E). Meanwhile, ELISA demonstrated that compared with the ICH+H₂O group, IL-1 β and TNF- α were decreased in the ICH+NAC group, and IL-10 was significantly increased (Fig. 4F–H). Briefly, ROS scavenger NAC inhibited the level of ROS, thereby inhibiting the inflammatory response mediated by NLRP3 inflammasome.

The Brain Injury After ICH Was Reduced by Silencing NLRP3

To explore the mechanism of NLRP3 on brain injury after ICH, we established a brain injury model after ICH, and treated the ICH model with silenced NLRP3. WB showed that compared with the ICH+sh-NC group, the protein levels of NLRP3, ASC, and caspase-1 in ICH+sh-NLRP3 group were clearly diminished (Fig. 5A). Compared with the ICH+sh-NC group, neurological damage, brain water content, number of degenerated neurons, apoptosis, and pathological severity were significantly decreased in the ICH+sh-NLRP3 group (Fig. 5B–G). Overall, silencing NLRP3 reduced brain injury after ICH.

DISCUSSION

ICH is considered the most serious subtype of stroke and often results in severe neurological dysfunction due to secondary cerebral edema [23]. Baicalein has been identified to promote neuron and behavior recovery after ICH by inhibiting cell apoptosis, oxidative stress, and neuroinflammation, and can be developed as a new drug for clinical treatment of ICH and ICH-related brain injury [3]. NLRP3 inflammasomes are responsible for sensing a variety of pathogenic and non-pathogenic injury signals and play an important role in neuroinflammation and neurological diseases [24]. In this paper, a brain injury model after ICH was successfully established and our results found that baicalein reduced the nervous system injury, lesion surface, brain water content, and apoptosis by inhibiting the ROS-NLRP3 inflammasome, thus alleviating the brain injury after ICH.

Baicalein can improve sports injury, reduce brain injury, and inhibit the production of pro-inflammatory cytokines and interleukin [25]. To explore the mechanism

of baicalein on brain injury after ICH, we established a model of brain injury after ICH by collagenase induction, and then the ICH model was treated by baicalein. Neural function and brain tissue water content are widely used to evaluate the degree of brain injury after ICH [26]. The results showed that after baicalein treatment, nervous system damage, lesion volume, and brain water content were decreased, cell apoptosis was decreased, the number of Nissl bodies was increased, and pathological severity was decreased. Consistently, previous reports supported that baicalein can provide neuroprotection in a variety of brain injury models [3, 27]. These results indicated that baicalein can ameliorate brain injury after ICH.

Oxidative stress is caused by the accumulation of ROS after ICH and leads to secondary damage to the brain tissue [28]. Next, the expression of ROS in brain tissues, and oxidative stress markers in serum of rats were determined. After baicalein treatment, MDA expression was decreased, and SOD and GSH-Px activities were significantly increased. A previous report has also shown that baicalein can significantly inhibit the production of ROS in lipopolysaccharide-activated BV-2 cells [29]. Briefly, the brain injury after ICH caused by excessive oxidative stress and inflammatory factors was inhibited by baicalein.

NLRP3 inflammasome is a key factor in ICH-induced inflammation [12]. ROS is critical for the activation of NLRP3 inflammasomes [15]. To further investigate whether baicalein inhibits brain injury after ICH by modulating NLRP3 inflammasome, we detected the expression of NLRP3, ASC, and caspase-1 in brain tissue of ICH rats, the levels of NLRP3, caspase-1, and IL-1 β , and the serum expression of inflammatory cytokines. The results showed that NLRP3 inflammasome was highly expressed in ICH. Baicalein inhibited the inflammatory cytokines and NLRP3 inflammasome. Baicalein has been reported to reduce acute liver injury by inhibiting NLRP3 inflammasomes [5]. Overall, baicalein may ameliorate brain injury after ICH by inhibiting the expression of NLRP3 inflammasome.

To identify the effect of ROS on NLRP3 inflammasomes, the ICH rat model was treated with ROS scavenger NAC. The results showed that the ROS scavenger NAC inhibited ROS levels and thus inhibited the inflammatory response mediated by NLRP3 inflammasomes. According to the reports, melatonin may play a direct or indirect role in anti-inflammatory and anti-apoptosis by reducing ROS levels in ICH [8]. Blocking the ROS/NLRP3 signaling helps inhibit

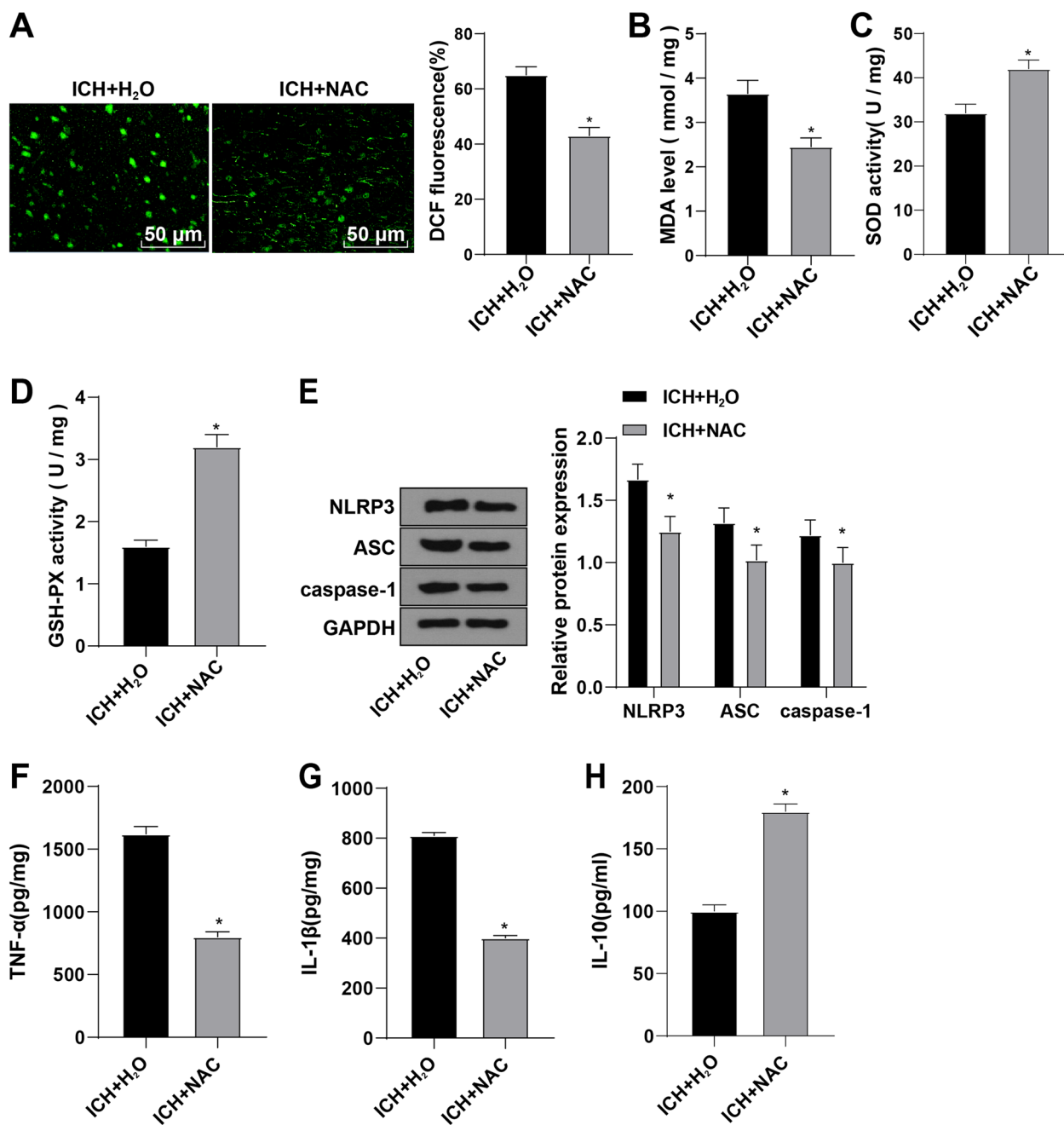


Fig. 4 ROS scavenging agent NAC inhibited NLRP3 inflammasome-mediated inflammation. ICH rats were injected with ROS scavengers (NAC) and H₂O was injected as control. **A** DCF fluorescence staining was used to detect ROS expression levels in brain tissues (magnification: ×200). **B–D** The expression levels of oxidative stress markers MDA, SOD, and GSH-Px in brain tissues were detected by ELISA. **E** WB was used to detect the protein levels of NLRP3, ASC, and caspase-1 in brain tissue. **F–H** The expression levels of inflammatory cytokines IL-1β, TNF-α, and IL-10 in brain tissues were detected by ELISA. Data were presented as mean ± standard deviation, and unpaired *t* test was used for comparison between two groups (*N* = 6). * compared with the ICH + H₂O group, *P* < 0.05.

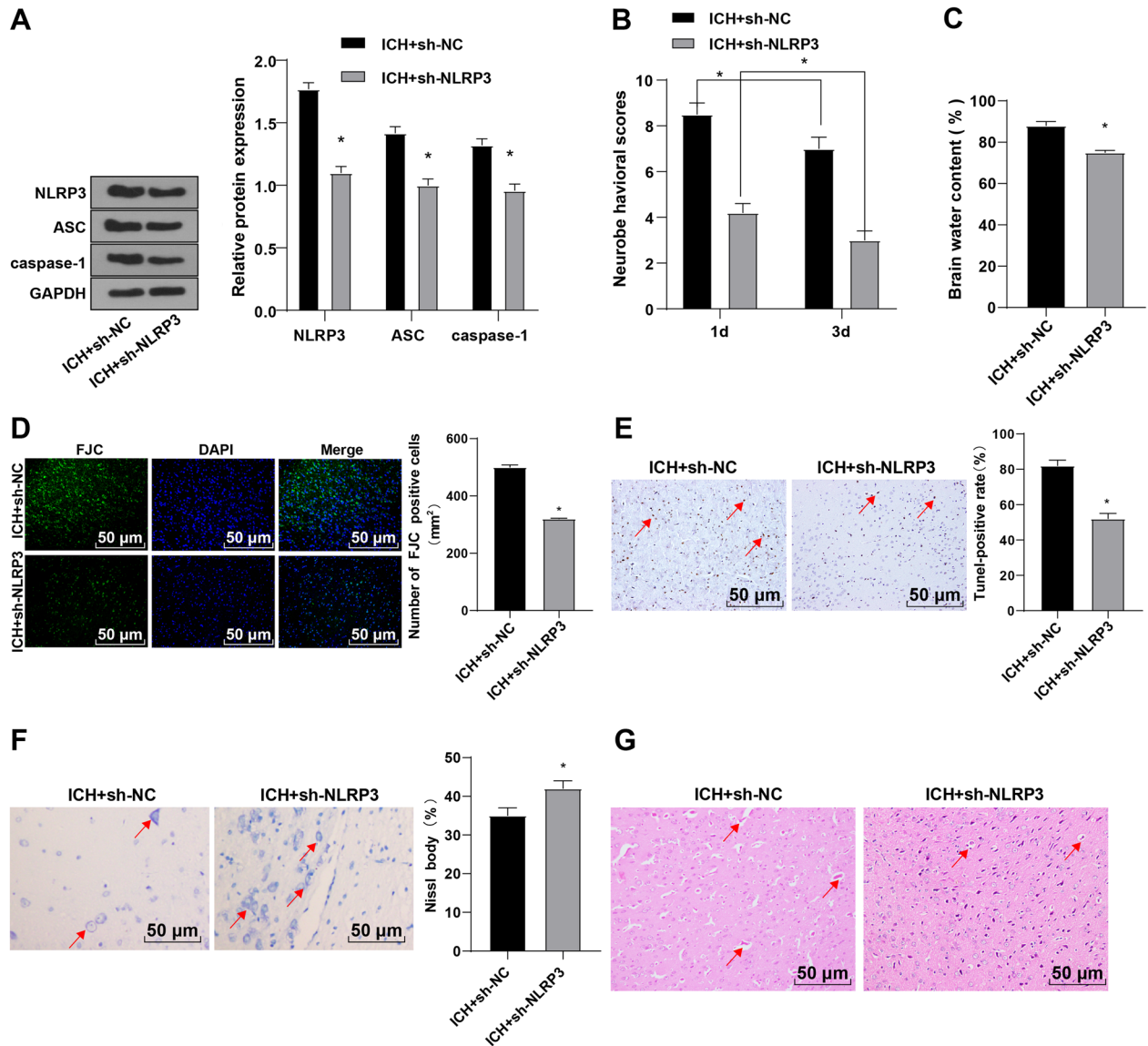


Fig. 5 Silencing NLRP3 reduced brain injury after ICH. **A** The protein levels of NLRP3, ASC, and Caspase-1 in brain tissues were detected by WB. **B** mNSS was used to score the neurological severity. **C** Brain water content measured as a percentage of wet/dry weight. **D** The number of degenerated neurons in brain tissue was detected by FJC staining (magnification: $\times 200$). **E** TUNEL staining was used to detect brain tissue apoptosis (magnification: $\times 200$, yellow-brown areas indicated by arrows represent TUNEL positive). **F** Nissl staining was used to detect the condition of Nissl bodies (magnification: $\times 200$, blue-purple areas indicated by arrows represent Nissl bodies positive). **G** HE staining was used to detect the pathological condition of brain tissue (magnification: $\times 200$, the areas indicated by arrows represent vacuoles, shrinkage, inflammatory cell infiltration in brain tissue). Data were presented as mean \pm standard deviation, and unpaired *t* test was used for comparison between two groups ($N=6$). * compared with the ICH+sh-NC group, $P < 0.05$.

LPS-induced inflammation and microglia activation [30]. Our conclusion is that the ROS scavenger NAC inhibited ROS levels and thus inhibited NLRP3 inflammasome-mediated inflammation. Finally, in order to

explore the mechanism of NLRP3 on brain injury after ICH, we treated the ICH model with silencing NLRP3, and the results showed that after silencing NLRP3, the nervous system injury, brain water content, degenerated

neurons, apoptosis, and pathological severity were significantly reduced. It has been shown that verbascoside inhibits the inflammatory response after ICH by inhibiting NLRP3 [31]. The results showed that silencing NLRP3 can reduce the brain injury after ICH.

In conclusion, baicalein can improve brain injury after ICH by inhibiting the ROS-NLRP3 inflammasome. However, due to the limited time and funds, this paper is not thorough enough. The exact process of action mechanism is still poorly understood. In future studies, we should conduct more experiments to further study the effect of baicalein on brain injury after ICH through the ROS-NLRP3 signaling pathway, so as to increase the credibility of results and apply the result to clinical practice. A latest study supports that dietary nutrition aids in the prevention and remediation of neurologic symptoms in stroke and targeting metabolism-epigenetics-immunity network will delineate a new blueprint for combating stroke [32]. This also provides a novel study direction for our future research.

SUPPLEMENTARY INFORMATION

The online version contains supplementary material available at <https://doi.org/10.1007/s10753-021-01569-x>.

AUTHOR CONTRIBUTION

XC is the guarantor of integrity of the entire study; XC and YZ contributed to the study concepts, study design, and definition of intellectual content; SSW contributed to the literature research; XC contributed to the manuscript preparation and XC contributed to the manuscript editing and review; SSW and WW contributed to the clinical studies; XC, YZ, SSW, and WW contributed to the experimental studies and data acquisition; XC and YZ contributed to the data analysis and statistical analysis. All the authors read and approved the final manuscript.

DATA AVAILABILITY

All the data generated or analyzed during this study are included in this published article.

DECLARATIONS

Ethics Approval Animal experiments followed the standards established by the animal experiment committee of the Fourth Affiliated Hospital of China Medical University and approved by the ethics committee of the

Fourth Affiliated Hospital of China Medical University. All animal experiments were conducted according to the “Guidelines for the Care and Use of Laboratory Animals.”

Consent for Publication Not applicable.

Conflict of Interest The authors declare no competing interests.

REFERENCES

1. Lin, X., H. Ye, F. Siaw-Debrah, S. Pan, Z. He, H. Ni, Z. Xu, K. Jin, Q. Zhuge, and L. Huang. 2018. AC-YVAD-CMK inhibits pyroptosis and improves functional outcome after intracerebral hemorrhage. *BioMed Research International* 2018: 3706047.
2. Lu, Q., R. Liu, P. Sherchan, R. Ren, et al. 2021. TREM (triggering receptor expressed on myeloid cells)-1 inhibition attenuates neuroinflammation via PKC (protein kinase C) delta/CARD9 (caspase recruitment domain family member 9) signaling pathway after intracerebral hemorrhage in mice. *Stroke* 52 (6): 2162–2173.
3. Wei, N., Y. Wei, B. Li, and L. Pang. 2017. Baicalein promotes neuronal and behavioral recovery after intracerebral hemorrhage via suppressing apoptosis, oxidative stress and neuroinflammation. *Neurochemical Research* 42 (5): 1345–1353.
4. Luo, X., Z. Yu, C. Deng, J. Zhang, G. Ren, A. Sun, S. Mani, Z. Wang, and W. Dou. 2017. Baicalein ameliorates TNBS-induced colitis by suppressing TLR4/MyD88 signaling cascade and NLRP3 inflammasome activation in mice. *Science and Reports* 7 (1): 16374.
5. Xiao, T., Y. Cui, H. Ji, L. Yan, D. Pei, and S. Qu. 2021. Baicalein attenuates acute liver injury by blocking NLRP3 inflammasome. *Biochemical and Biophysical Research Communications* 534: 212–218.
6. Rui, W., S. Li, H. Xiao, M. Xiao, and J. Shi. 2020. Baicalein attenuates neuroinflammation by inhibiting NLRP3/caspase-1/GSDMD pathway in MPTP induced mice model of Parkinson’s disease. *Int J Neuropsychopharmacol*.
7. Li, D., G. Shi, J. Wang, D. Zhang, Y. Pan, H. Dou, and Y. Hou. 2019. Baicalein ameliorates pristane-induced lupus nephritis via activating Nrf2/HO-1 in myeloid-derived suppressor cells. *Arthritis Research & Therapy* 21 (1): 105.
8. Tang, J., R. Chen, L. Wang, L. Yu, D. Zuo, G. Cui, and X. Gong. 2020. Melatonin attenuates thrombin-induced inflammation in BV2 cells and then protects HT22 cells from apoptosis. *Inflammation* 43 (5): 1959–1970.
9. Chen, M. Y., X. J. Ye, X. H. He, and D. Y. Ouyang. 2021. The signaling pathways regulating NLRP3 inflammasome activation. *Inflammation*.
10. Liu, X., M. Zhang, H. Liu, R. Zhu, et al. 2021. Bone marrow mesenchymal stem cell-derived exosomes attenuate cerebral ischemia-reperfusion injury-induced neuroinflammation and pyroptosis by modulating microglia M1/M2 phenotypes. *Experimental Neurology* 341: 113700.
11. Zhu, F., L. Wang, Z. Gong, Y. Wang, Y. Gao, W. Cai, and J. Wu. 2021. Blockage of NLRP3 inflammasome activation ameliorates

- acute inflammatory injury and long-term cognitive impairment induced by necrotizing enterocolitis in mice. *Journal of Neuroinflammation* 18 (1): 66.
12. Wang, L., S. Zheng, L. Zhang, H. Xiao, H. Gan, H. Chen, X. Zhai, P. Liang, J. Zhao, and Y. Li. 2020. Histone deacetylation 10 alleviates inflammation after intracerebral hemorrhage via the PTPN22/NLRP3 pathway in rats. *Neuroscience* 432: 247–259.
 13. Xiao, L., H. Zheng, J. Li, Q. Wang, and H. Sun. 2020. Neuroinflammation mediated by NLRP3 inflammasome after intracerebral hemorrhage and potential therapeutic targets. *Molecular Neurobiology* 57 (12): 5130–5149.
 14. Kim, H., J.E. Lee, H.J. Yoo, J.H. Sung, and S.H. Yang. 2020. Effect of pioglitazone on perihematomal edema in intracerebral hemorrhage mouse model by regulating NLRP3 expression and energy metabolism. *Journal of Korean Neurosurgical Association* 63 (6): 689–697.
 15. Zhao, Y., S. Jiang, J. Zhang, X.L. Guan, B.G. Sun, and L. Sun. 2021. A virulent *Bacillus cereus* strain from deep-sea cold seep induces pyroptosis in a manner that involves NLRP3 inflammasome, JNK pathway, and lysosomal rupture. *Virulence* 12 (1): 1362–1376.
 16. Zhao, M., J. Gao, C. Cui, Y. Zhang, X. Jiang, and J. Cui. 2021. Inhibition of PTEN ameliorates secondary hippocampal injury and cognitive deficits after intracerebral hemorrhage: Involvement of AKT/FoxO3a/ATG-mediated autophagy. *Oxidative Medicine and Cellular Longevity* 2021: 5472605.
 17. Sun, Z., K. Wu, L. Gu, L. Huang, Q. Zhuge, S. Yang, and Z. Wang. 2020. IGF-1R stimulation alters microglial polarization via TLR4/NF-kappaB pathway after cerebral hemorrhage in mice. *Brain Research Bulletin* 164: 221–234.
 18. Shen, R., P. Yin, H. Yao, L. Chen, X. Chang, H. Li, and X. Hou. 2021. Punicalin ameliorates cell pyroptosis induced by LPS/ATP through suppression of ROS/NLRP3 pathway. *Journal of Inflammation Research* 14: 711–718.
 19. Chen, J., Y. Li, L. Wang, Z. Zhang, D. Lu, M. Lu, and M. Chopp. 2001. Therapeutic benefit of intravenous administration of bone marrow stromal cells after cerebral ischemia in rats. *Stroke* 32 (4): 1005–1011.
 20. Omolaoye, T.S., B.T. Skosana, and S.S. du Plessis. 2018. Diabetes mellitus- induction: Effect of different streptozotocin doses on male reproductive parameters. *Acta Histochemica* 120 (2): 103–109.
 21. Livak, K.J., and T.D. Schmittgen. 2001. Analysis of relative gene expression data using real-time quantitative PCR and the 2(-delta delta C(T)) method. *Methods* 25 (4): 402–408.
 22. Ji, Y., J. Han, N. Lee, J. H. Yoon, K. Youn, H. J. Ha, E. Yoon, D. H. Kim, and M. Jun. 2020. Neuroprotective effects of baicalein, wogonin, and oroxylin A on amyloid beta-induced toxicity via NF-kappaB/MAPK pathway modulation. *Molecules* 25 (21): 4600.
 23. Chen, M., L. Lai, X. Li, X. Zhang, et al. 2016. Baicalein attenuates neurological deficits and preserves blood-brain barrier integrity in a rat model of intracerebral hemorrhage. *Neurochemical Research* 41 (11): 3095–3102.
 24. Mishra, S. R., K. K. Mahapatra, B. P. Behera, S. Patra, et al. 2021. Mitochondrial dysfunction as a driver of NLRP3 inflammasome activation and its modulation through mitophagy for potential therapeutics. *The International Journal Biochemistry & Cell Biology* 136: 106013.
 25. Zhang, X., Y. Yang, L. Du, W. Zhang, and G. Du. 2017. Baicalein exerts anti-neuroinflammatory effects to protect against rotenone-induced brain injury in rats. *International Immunopharmacology* 50: 38–47.
 26. Zhou, W., G. Huang, J. Ye, J. Jiang, and Q. Xu. 2020. Protective effect of miR-340-5p against brain injury after intracerebral hemorrhage by targeting PDCD4. *Cerebrovascular Diseases* 49 (6): 593–600.
 27. Wang, C.X., G.B. Xie, C.H. Zhou, X.S. Zhang, et al. 2015. Baicalein alleviates early brain injury after experimental subarachnoid hemorrhage in rats: Possible involvement of TLR4/NF-kappaB-mediated inflammatory pathway. *Brain Research* 1594: 245–255.
 28. Yao, Z., Q. Bai, and G. Wang. 2021. Mechanisms of oxidative stress and therapeutic targets following intracerebral hemorrhage. *Oxidative Medicine and Cellular Longevity* 2021: 8815441.
 29. Yan, J. J., G. H. Du, X. M. Qin, and L. Gao. 2020. Baicalein attenuates the neuroinflammation in LPS-activated BV-2 microglial cells through suppression of pro-inflammatory cytokines, COX2/NF-kappaB expressions and regulation of metabolic abnormality. *International Immunopharmacology* 79:106092.
 30. Bian, H. T., G. H. Wang, J. J. Huang, L. Liang, L. Xiao, and H. L. Wang. 2020. Scutellarin protects against lipopolysaccharide-induced behavioral deficits by inhibiting neuroinflammation and microglia activation in rats. *International Immunopharmacology* 88: 106943.
 31. Zhou, H., C. Zhang, and C. Huang. 2021. Verbascoide Attenuates acute inflammatory injury caused by an intracerebral hemorrhage through the suppression of NLRP3. *Neurochemical Research* 46 (4): 770–777.
 32. Mao, X. Y., X. X. Yin, Q. W. Guan, Q. X. Xia, N. Yang, H. H. Zhou, Z. Q. Liu, and W. L. Jin. 2021. Dietary nutrition for neurological disease therapy: Current status and future directions. *Pharmacology & Therapeutics* 226: 107861.

Publisher's Note Springer Nature remains neutral with regard to jurisdictional claims in published maps and institutional affiliations.